The Role of Site Conditions on the Structural Damage in the City of Valdivia during the 22 May 1960 M_w 9.5 Megathrust Chile Earthquake

César Pastén[*1], Felipe Campos[2], Felipe Ochoa-Cornejo[1], Sergio Ruiz[3], Galo Valdebenito[4], David Alvarado[4], Felipe Leyton[5], and Ricardo Moffat[6]

Abstract

The 22 May 1960 M_w 9.5 Valdivia megathrust earthquake, with a rupture length close to 1000 km in the central–south Chile, is the largest recorded earthquake in the modern times. The city of Valdivia is located about 300 km south of the northern boundary of the rupture in front of one of the largest asperities of the earthquake. In this article, we analyze the geology of the city and results from geophysical exploration methods that could explain the observed pattern of structural earthquake-induced damage. Surface waves methods results indicate that the soils in Valdivia have shear-wave velocity in the upper 30 m V_{S30} ranging from 150 to 300 m/s, whereas horizontal-to-vertical spectral ratios (HVSRs) calculated from ambient seismic noise show predominant vibration periods between 0.6 and 1.4 s. The housing stock in Valdivia at the time of the earthquake mainly consisted of one- and two-story wooden buildings, and fewer masonry and reinforced-concrete buildings. Our reinterpretation of the data indicates that despite the large seismic demand and the low shear-wave velocities, well-designed, well-constructed, and founded structures were barely damaged. Most of the structural damage concentrated in hybrid structural systems, poorly designed and constructed structures, and structures with deficient foundations build over uncontrolled backfills that experienced lateral movement and differential settlement. The predominant vibration periods from the HVSR do not correlate with the most damaged areas, but it seems to correlate with the depth of the soil deposit. The reduced damage of the larger structures in the city at the time of the earthquake may be partially explained because their vibration periods did not resonate with the predominant vibration period of the soil, in addition to their large structural redundancy.

Cite this article as Pastén, C., F. Campos, F. Ochoa-Cornejo, S. Ruiz, G. Valdebenito, D. Alvarado, F. Leyton, and R. Moffat (2021). The Role of Site Conditions on the Structural Damage in the City of Valdivia during the 22 May 1960 M_w 9.5 Megathrust Chile Earthquake, *Seismol. Res. Lett.* **XX**, 1–15, doi: 10.1785/0220190321.

Supplemental Material

Introduction

On 22 May 1960 at 19:11:17 (UTC), the largest earthquake ever recorded in the modern times ruptured about 1000 km off the coast of central–south Chile (Press *et al.*, 1961; Kanamori, 1977, Fig. 1). The interplate 1960 M_w 9.5 Chilean earthquake generated tsunami waves that reached the coasts of Japan, Hawaii, Peru, and Alaska (Cox and Mink, 1963; Keys, 1963; Vitousek, 1963; Abe, 1979) and caused high-seismic intensities in different cities along the central–south Chile (Saint-Amand, 1961a; Alvarez, 1963; Galli and Sánchez, 1963a,b,c; B. Y. H. Thomas *et al.*, 1963a,b; H. Thomas *et al.*, 1963; Astroza and Lazo, 2010). Coseismic slip models, obtained from uplift and subsidence reported by Plafker and Savage (1970) and tsunami inferences, indicate that the rupture of the earthquake developed from the Arauco Peninsula to the south of the Chiloe Island (Barrientos and Ward, 1990; Moreno *et al.*, 2009; Fujii and Satake, 2013; Ho *et al.*, 2019). One of the closest cities to the main earthquake asperities was the city of Valdivia, located on a complex basin crossed by fluvial deposits (Figs. 1 and 2). The city had nearly 57,000 inhabitants at the time of the earthquake, with a developed commercial district and the residential area over the south bank of the Calle-Calle River. The north bank of the river, called

1. Department of Civil Engineering, University of Chile, Santiago, Chile, https://orcid.org/0000-0002-6683-0619 (CP); 2. Advanced Mining Technology Center, University of Chile, Santiago, Chile; 3. Department of Geophysics, University of Chile, Santiago, Chile, https://orcid.org/0000-0003-1758-0788 (SR); 4. Núcleo de Investigación en Riesgos Naturales y Antropogénicos RiNA, Universidad Austral de Chile, Valdivia, Chile, https://orcid.org/0000-0003-1872-9484 (GV); 5. National Seismological Center, University of Chile, Santiago, Chile, https://orcid.org/0000-0002-6438-4045 (FL); 6. Facultad de Ingeniería y Ciencias, Universidad Adolfo Ibañez, Santiago, Chile, https://orcid.org/0000-0002-9301-6030 (RM)

*Corresponding author: cpasten@uchile.cl

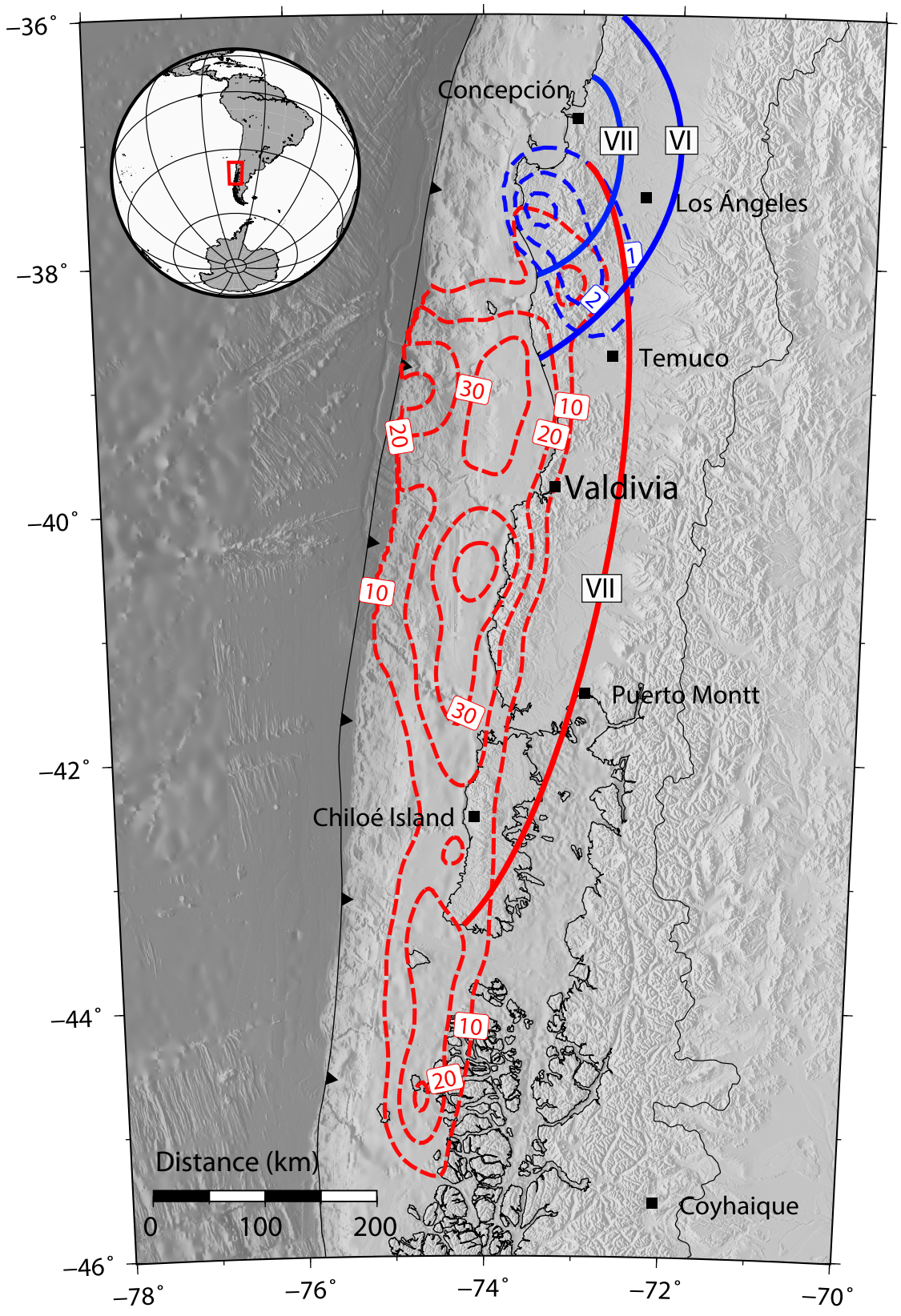

Figure 1. The 1960 Chilean earthquakes in central–south Chile. Segmented lines are iso-contours corresponding to the slip (in meters) of the 21 May M_w 8.1 Concepción earthquake (blue) and the 22 May M_w 9.5 Valdivia earthquake (red). Continuous lines are the Medvedev–Sponheuer–Karnik isoseismal intensities of the Concepción earthquake (blue) and the Valdivia megathrust earthquake (red). The city of Valdivia is also indicated. The inset details the area shown in this figure in the context of South America. The color version of this figure is available only in the electronic edition.

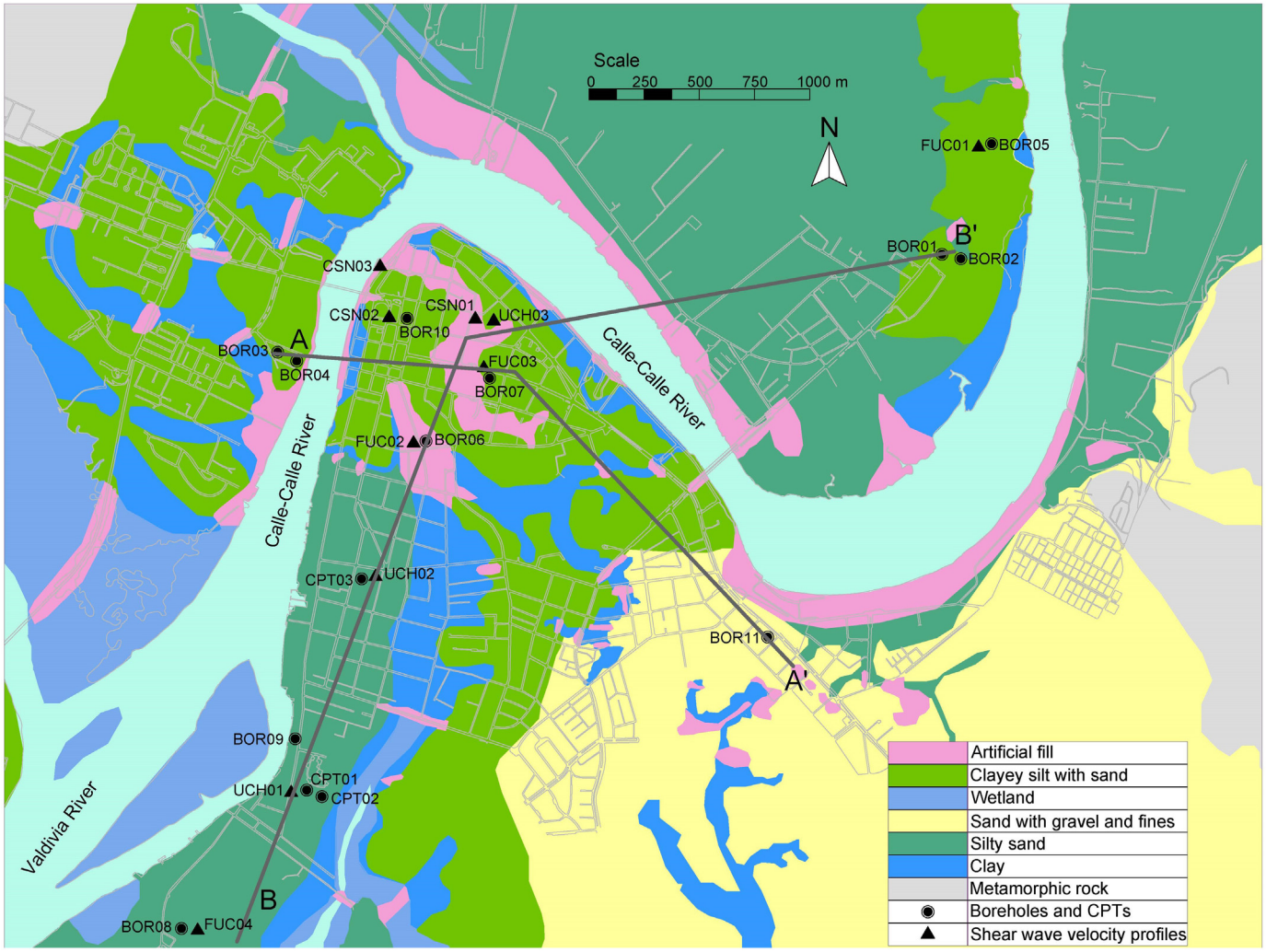

Figure 2. Surface geology of the city of Valdivia; cross sections A–A′ and B–B′ are shown in Figure 3. CPT, cone penetration test. The color version of this figure is available only in the electronic edition.

Las Animas, had fewer residences and properties of importance. Across the Calle-Calle River, on the eastern side of Isla Teja, there were houses, factories, and a large university campus. The rest of the area was utilized for agriculture.

Despite the large magnitude earthquake and complex soil behavior of the Valdivia basin, some structures were not damaged during this event, in contrast with other structures that were completely destroyed. In this work, we study the observed pattern of structural earthquake-induced damage and its relationship with the local geology, site effects deduced from our geophysical measurement campaigns, and geotechnical characterization of the foundation soil to understand the triggering factors of most of the damage in the city of Valdivia during the 22 May 1960 megathrust earthquake. This study provides relevant information to understand the seismic risk of coastal megacities located in subduction zones where giant megathrust earthquakes can occur.

Regional Structural Damage of the 1960 Valdivia Earthquakes

The M_w 9.5 Valdivia earthquake of 22 May 1960 (Kanamori and Cipar, 1974) was preceded by a large event of magnitude M_w 8.1 that occurred on 21 May at 10:02:52 UTC just north of the M_w 9.5 rupture zone, close to the city of Concepción (Cifuentes, 1989; Ruiz and Madariaga, 2018; Ojeda *et al.*, 2020). This former event caused Medvedev–Sponheuer–Karnik (MSK) intensities that show a damaged area of nearly 300 km with larger intensities toward the north. In contrast, the 22 May earthquake revealed a damaged area of almost 800 km long, according to Astroza and Lazo (2010), who compiled information from damage reports and newspapers of the date. Figure 1 shows the MSK isoseismal intensities of the 21 and 22 May earthquakes.

The city of Valdivia was strongly affected by the tsunami in some places close to the Calle-Calle River (Sievers *et al.*, 1963), and several houses were destroyed by the 22 May earthquake, whereas other civil structures suffered no damage. A witness of the 22 May earthquake in the city of Valdivia reported high-frequency ground motion and two distinctive peak ground

shakings (Labbé, 2019). Valdivia did not suffer structural damage associated with the 21 May earthquake (Astroza and Lazo, 2010). In central–south Chile, other large magnitude earthquakes preceded the 1960 M_w 9.5 Valdivia, with events of similar magnitudes occurring at least 400 yr ago (Cisternas *et al.*, 2005, 2017; Ruiz and Madariaga, 2018). During these precedent earthquakes, the city of Valdivia only consisted of few houses, and it is not possible to perform an analysis similar to the one shown herein for the 1960 event.

Geological Framework

The city of Valdivia is located in the basin of the Valdivia River, separated from the Tolten River by a transverse range of hills and by a chain of coastal hills that form a range of nearly 600 m in altitude toward the south, continuing southward to the Altos del Mirador at about 300 m above sea level (m.a.s.l.). This range is crossed by the Valdivia River in front of the coastal town of Corral. Toward the southeast of the city of Valdivia, the hill Huichahue (640 m) slopes toward the valley of the Valdivia River and defines the course of the Futa and the Angachilla Rivers (Arenas *et al.*, 2005).

The city of Valdivia developed on a terrace dissected by ancient channels, many of which are no longer active U-shape channels, and currently filled with alluvium and artificial fill. Almost the entire valley was covered by this terrace, as indicated by remnants in other parts of the city. The city is crossed by the Calle-Calle River that flows from north to south, as well as the Valdivia, the Cau-Cau, and the Cruces Rivers (Fig. 2). The geological units in the main bank of the city are described next.

Inorganic silt

Inorganic silt is the shallower stratum found in the area, corresponding to a soil used in agriculture with a thickness varying from 0.5 to 3.5 m. The stratum consists of three layers, the shallower one is a coffee-colored black silt with some organic matter; the intermediate one has sand and clay; and the lower one has high clay content due to leaching of the upper layers. There is evidence that this is an aeolian deposit (Doyel *et al.*, 1963). It is not a proper foundation soil due to its high compressibility (Barozzi and Lemke, 1966). Given the reduced thickness of the stratum, it is not considered in the geologic map in Figure 2.

Clayey silt with sand

This unit consists of dark coffee to white clays, sands, clayey sands, and silts. The clays vary from plastic to friable and some are laminated. The sands are in general fine-to-medium grained. Part of these sands are completely indurated and composed of fragments of volcanic rocks and granites, cemented by palagonite. Two horizons have been tentatively identified. The unit has an irregularly eroded surface, the thickness varying from 0.5 to 2 m, and the base of the unit is between 7 and 7.5 m, whereas the ceil is between 8 and 9 m.a.s.l.. This material is locally known as "Cancagua" and it is mainly located in the central and east part of the city. Cancagua is an estuarine complex developed during the last glacial cycle's highstand that continued accumulating sediments during a substantial part of the falling stage (Vega *et al.*, 2018). The water table is usually below this unit. This unit forms terraces between 8 and 15 m.a.s.l., whose high stiffness makes it a proper foundation soil for houses and small buildings.

Silty sand

This unit of recent sediments consists of gray olive to moderate gray medium silty sand with angular to subrounded grains, and layers of materials with high content of organic matter. The grains are andesitic basaltic rocks, micaceous shale, quartz grains, feldspar, and some glass. It is found mainly in the margins of the current course of the Calle-Calle River. The maximum thickness is unknown, but it is believed to be thicker than 30 m. It has relatively high permeability, and the water table during the summer season varies from 0.5 to 2 m below the surface. This material becomes soft upon saturation, which makes it a poor foundation material (Arenas *et al.*, 2005).

Clay

This unit of swamps and recent fluvial materials consists of clays and silts of high water content and organic matter, as well as interbedded sand layers. The materials classify from organic clayey silt to organic clay of medium plasticity. The clays range from light gray olive to yellowish dark brown. It contains several fragments of palecypod shells (mytilus) and wood. Deeper than 10 m, the voids of the unit are filled with highly flammable swamp gas. This unit outcrops in the southwest of the city in areas exposed to floodings, and it has been identified in boreholes underlying the silty sand unit. The thickness of the unit is unknown, but it is believed that it can be thicker than 30 m. The unit has low permeability and the water table in the summer season is at the surface or above in some swampy areas. Because of the low consistency and high water content, usually larger than the liquid limit, this material is only a proper foundation soil for lightweight structures or structures founded on piles.

Silt, clay, and silty sand

This unit consists of lenses of silt and clay that alternate with lenses of silty sand. The classification of the material can vary from organic silt (OL), medium plasticity clay (OH), and fine sand to coarse silt (SM). The color varies from light to dark gray to black. Some clays are finely laminated. It can be found in the entire study area underlying other sedimentary units, such as the clay and the silty sand units (Fig. 3). The thickness can reach more than 10 m, but the depth of the base is unknown. It has low permeability and the groundwater table is usually few meters below its roof. The high overconsolidation of this unit, mainly in the lower part, makes it stiff and a good foundation soil (Barozzi and Lemke, 1966).

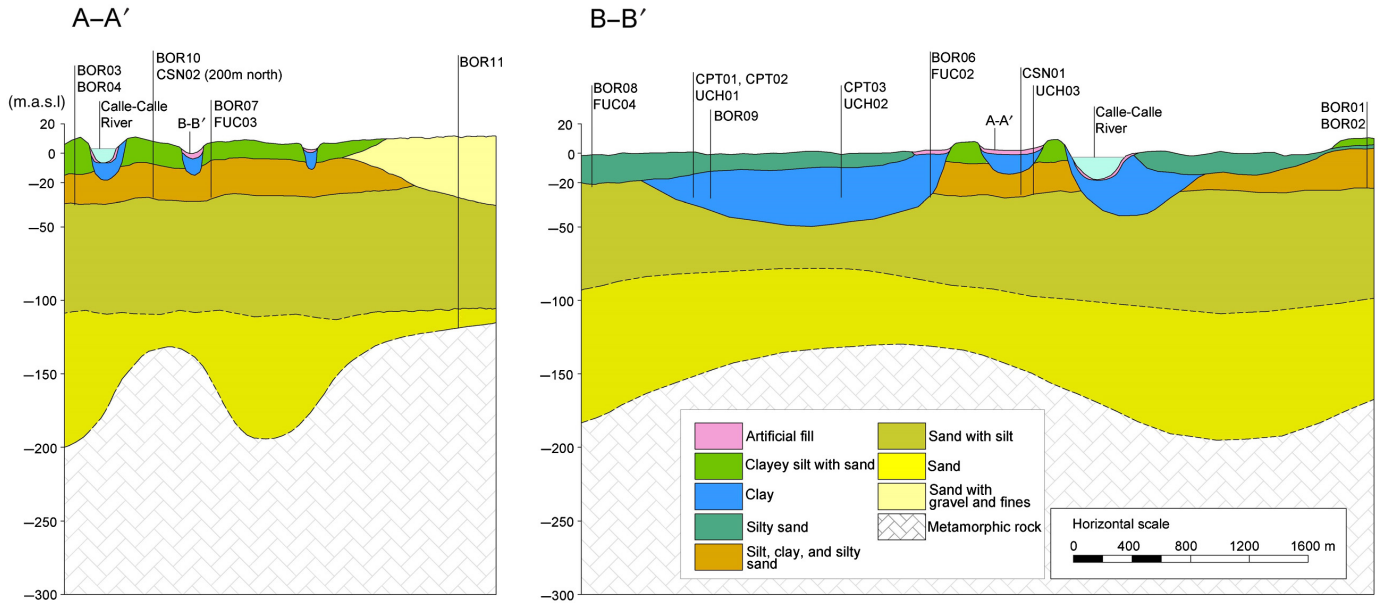

Figure 3. Cross sections of the city of Valdivia shown in Figure 2. The color version of this figure is available only in the electronic edition.

Sand with gravel and fines

This is a fluvio-glacial material that consists of layers of fine to coarse sand with some gravel and clayey silts. The material classifies as well-graded sand with some gravel, silt, and clay. The gravel fraction represents less than 10% and the maximum particle size is about 7 cm of subangular clasts of granite and metamorphic rocks (Barozzi and Lemke, 1966). It is a well-consolidated material with the upper layers lightly cemented with limonite and irregularly eroded between 6 and 12 m.a.s.l. (Doyel *et al.*, 1963). It can be found in the east side of the city overlaying the unit composed of silt, clay, and silty sand and almost entirely covered by the inorganic silt unit. The thickness of the unit is believed to be larger than 30 m, according to recollected information from boreholes (Barozzi and Lemke, 1966). This unit has moderate permeability and the water table is between 5 and 8 m below the surface. These materials are compact and hence they represent a suitable foundation soil along with the clayey silt with sand unit.

Artificial fill

This material consists of recent alluvium and artificial fill of variable thickness and composition. The alluvium fraction is gray to white plastic clay, black to white sands, interbedded with yellow silts and fragments of marine shells. It presents artificial fill, debris, and trash, such as wood, gravel, and rocks (Doyel *et al.*, 1963). The unit mainly covers the low parts of the city, it has high water content, and it is highly compressible due to the slight compaction. The thickness varies from few centimeters to 9 m in some embankments.

Cross Sections along the City of Valdivia

Combining the geological and geotechnical information summarized in the Geological Framework section, we constructed two representative cross sections of the city of Valdivia. To the authors' best knowledge, the only borehole that has reached the metamorphic basement rock in the city at 130 m depth is BOR11 in Figures 2 and 3 (Doyel *et al.*, 1963). Based on this threshold depth, we extended the cross sections down to the bedrock, with additional information provided from the maps developed by Barozzi and Lemke (1966) and Arenas *et al.* (2005).

We also constructed typical shear-wave velocity profiles of the main geological units in the city of Valdivia (Fig. 4), following the ambient noise cross-correlation method developed in Pastén *et al.* (2016). The method defines the dispersion curve from the zero-crossings of the coherency function calculated from the vertical components of ambient noise recorded by pairs of triaxial seismographs. The inversion process was performed using the Geopsy software (Wathelet, 2005) following the methodology in Leyton *et al.* (2018). Additional information, such as borehole stratigraphies and seismic cone penetration tests (sCPTs) results (American Society for Testing and Materials [ASTM], 2012), was used to constrain the inversion process.

The profile UCH01 over the silty sand unit (Fig. 1) shows a constant shear-wave velocity of 160 m/s for the shallower silty sand and the underlying clay layer. This value was confirmed with sCPT results performed up to 30 m depth. In addition to a low shear-wave velocity, the underlying clay has a very low tip resistance (<2 MPa) from 20 to 30 m depth, according to sCPT measurements. According to the Chilean earthquake resistant design standard for buildings (Instituto Nacional de Normalización [INN], 2012), the site classifies as type E (V_{S30} < 180 m/s). The profile CSN01 over the artificial fill

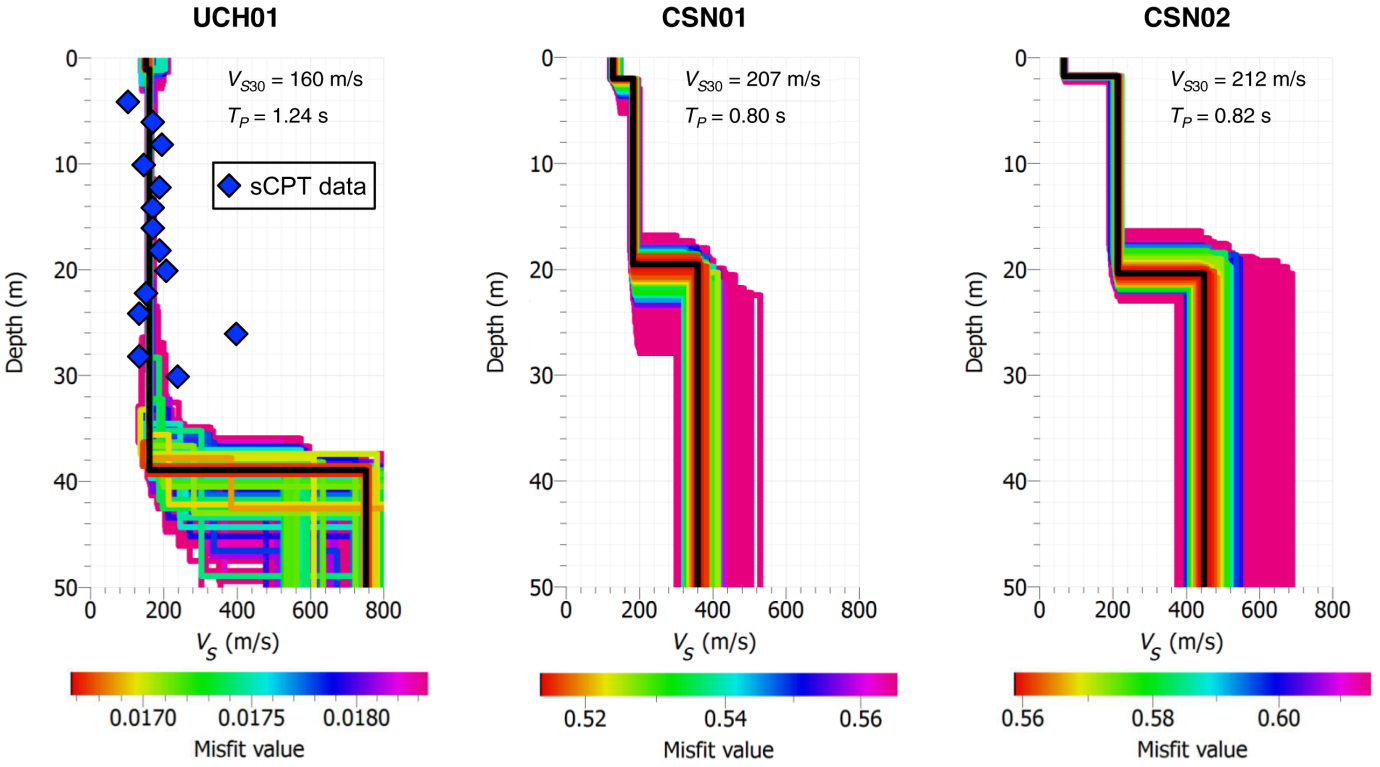

Figure 4. Shear-wave velocity profiles of representative sites in the city of Valdivia obtained with surface-wave methods. Diamonds in profile UCH01 are shear-wave velocities measured with the seismic CPT (sCPT). Locations of the sites are shown in Figures 2 and 3. Profiles in black are those with the lowest misfits in the inversion process. Profiles in color have misfits 10% larger than the minimum value, according to the color bar. The color version of this figure is available only in the electronic edition.

recognizes three layers associated with the shallower artificial fill ($V_S = 120$ m/s), the clay ($V_S = 180$ m/s), and the silt–clay–silty sand unit ($V_S = 350$ m/s). This soil profile classifies as soil type D (180 m/s $< V_{S30} = 207$ m/s < 350 m/s). The profile CSN02 measured over the clayey silt with sand unit shows three layers and classifies as soil type D (180 m/s $< V_{S30} = 212$ m/s < 350 m/s). Figure 4 shows that shear-wave velocity variability is low in the upper 15 m but increases deeper than 35 m in profile UCH01 and deeper than 20 in profiles CSN01 and CSN02. The larger uncertainty with depth in the V_S values and the depth of the velocity changes is related to the soils underneath the shallower clay and clayey silt with sand materials shown in Figure 3.

Earthquake-Induced Damage in the City of Valdivia

In this study, we reinterpret the earthquake-induced structural damage reported by Watanabe and Karzulovic (1960), Cambiazo (1961), Saint-Amand (1961b), Duke and Leeds (1963), and Steinbrugge and Flores (1963). The structural damage and the stock of structures in the city of Valdivia at the time of the earthquake was complemented by studies by Weischet (1963), Barozzi and Lemke (1966), and Lástrico (1967). The most common types of structures at the time were one- and two-story wood-frame houses, which were usually protected with exterior metal sheets to withstand the harsh weather conditions in the zone. The types of structures that followed were one- and two-story masonry buildings. These structures varied from unconfined to confined masonry, and displayed in some cases hybrid construction systems mixed with wood. Finally, there were reinforced-concrete buildings constructed mainly from the beginning of the twentieth century, some of which were steel-concrete based, and newer buildings from 1930 to 1950 s, such as the Cervantes Building (completed in 1935), the Regional Hospital (opened in 1939), the Prales building, the Traumatology Hospital (also known as Orthopedic Hospital), and the Pedro de Valdivia Hotel (Steinbrugge and Flores, 1963; Labbé, 2019).

The cause of structural failure can be attributed to several factors. Reinforced-concrete structures, structures build with brick masonry with reinforced-concrete columns and reinforced-concrete tie beams (usually not reinforced within the brick panel wall) and reinforced hollow concrete blocks performed adequately when well designed and well constructed with proper materials (Steinbrugge and Flores, 1963). Many unreinforced brick masonry buildings experienced extensive damage; however, structures with interior cross walls tied to the exterior brick masonry walls suffered no apparent damage. The damage in reinforced-concrete structures, such as the Regional Hospital, the Traumatology Hospital, and elevated water tanks, was caused by deficient structural design and

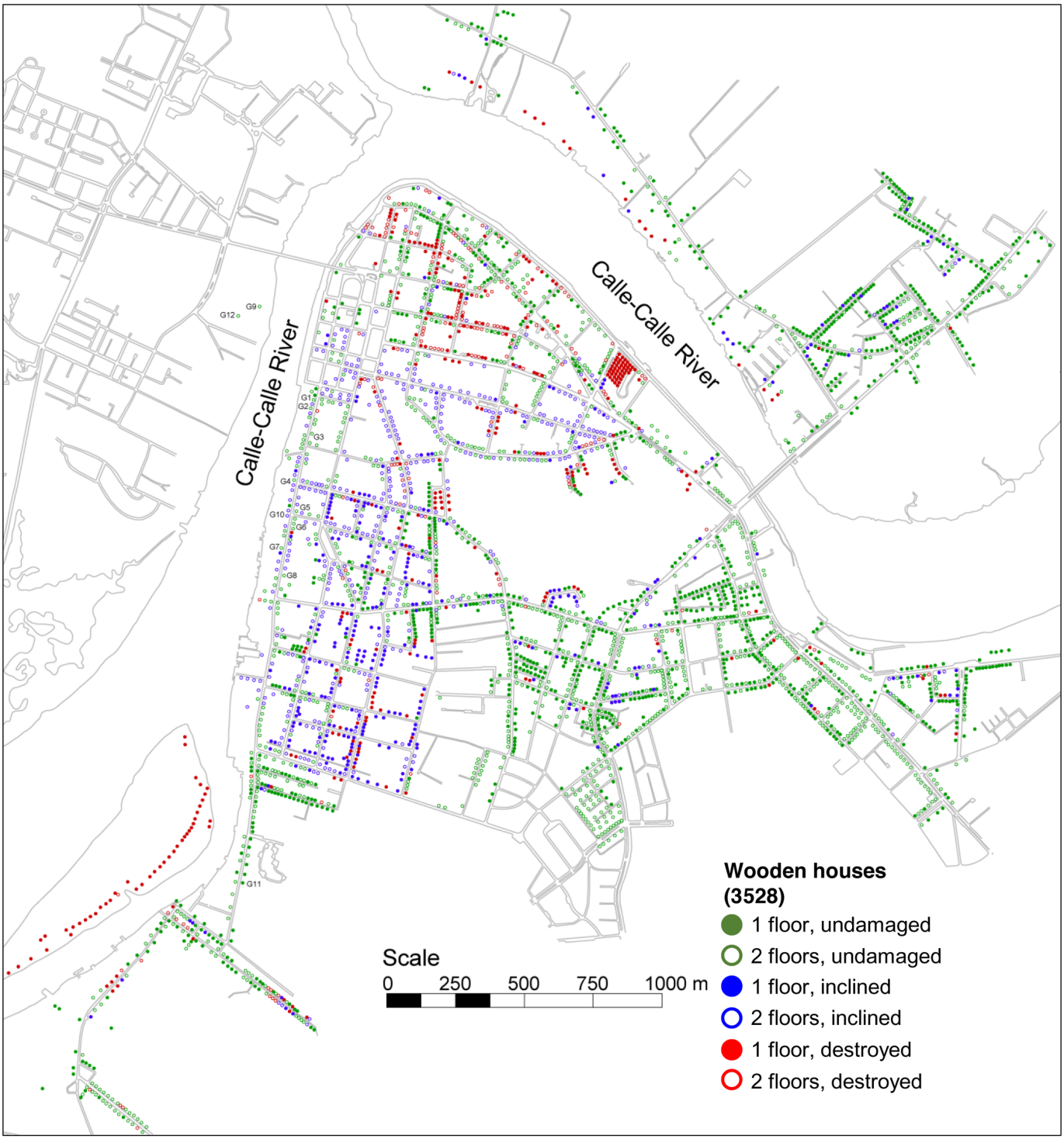

construction problems (Steinbrugge and Flores, 1963). The Regional Hospital was a complex of seven structures of reinforced concrete, one of the largest structures in the city. This structure suffered severe damage due to its irregular shear walls, pounding between structures, and construction problems (Steinbrugge and Flores, 1963).

In general, wooden houses performed well during the earthquake. The failure of wood-frame structures was caused

Figure 5. Wooden houses undamaged, inclined, and damaged during the 22 May 1960 Chile earthquake (data from Weischet, 1963; Barozzi and Lemke, 1966; Lástrico, 1967). The location of the 12 undamaged German-style wooden houses are indicated as G1–G12. The color version of this figure is available only in the electronic edition.

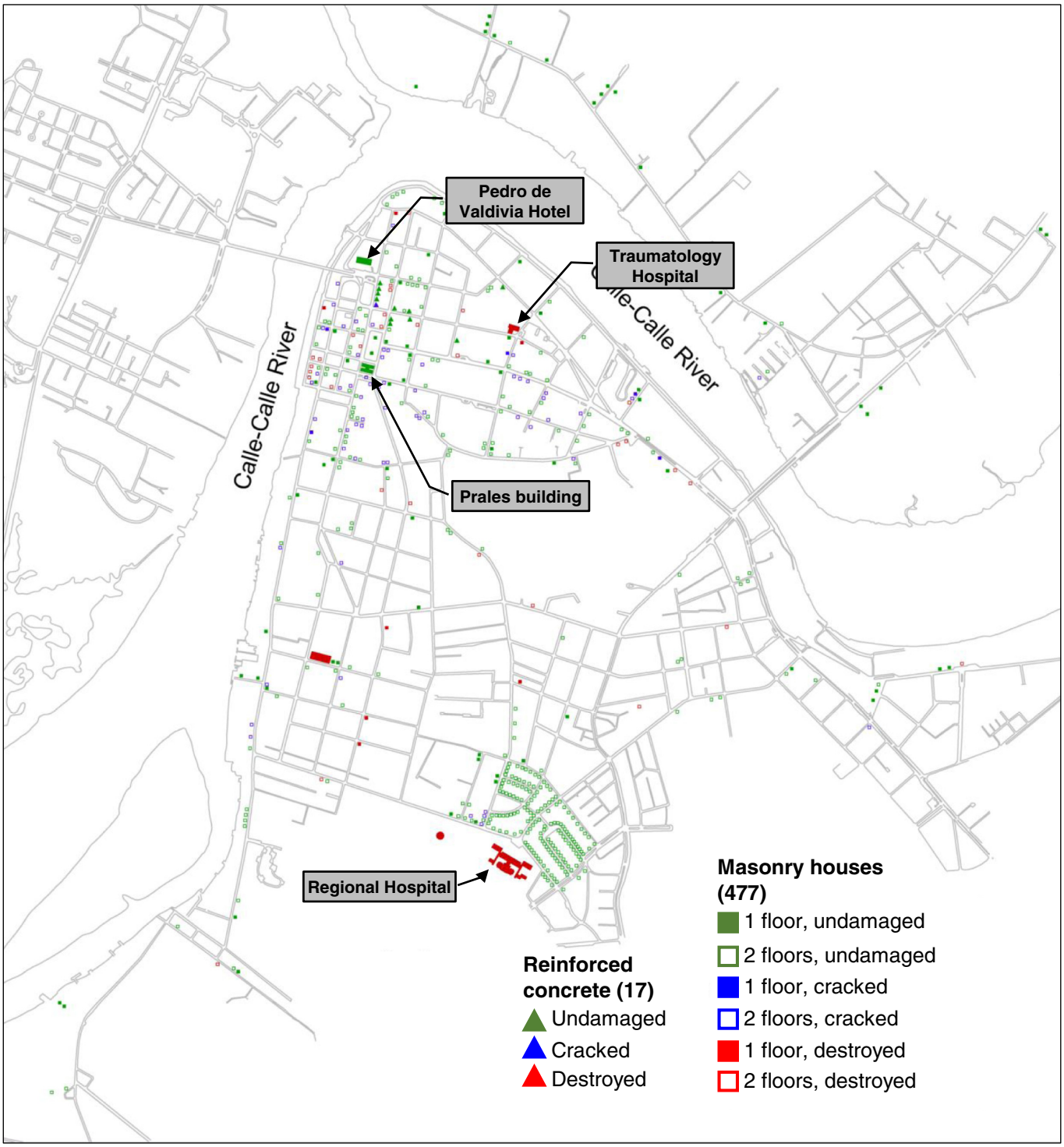

Figure 6. Masonry houses and reinforced-concrete structures undamaged, cracked, and damaged during the 22 May 1960 Chile earthquake (data from Weischet, 1963; Barozzi and Lemke, 1966; Lástrico, 1967). The color version of this figure is available only in the electronic edition.

by construction quality problems, such as insufficient nails and poor maintenance of the foundation system in the highly humid Valdivia climate. Wood-frame structures with lightly reinforced-concrete or unreinforced-masonry partitions or exterior walls behaved poorly. For instance, the unbraced reinforced-concrete firewalls on property lines between wooden buildings often fell, destroying or severely damaging the adjoining wood-frame houses (Steinbrugge and Flores, 1963).

Figures 5 and 6 show the distribution of wooden and masonry houses in the city, respectively. Each figure indicates houses of one story and two stories that were undamaged,

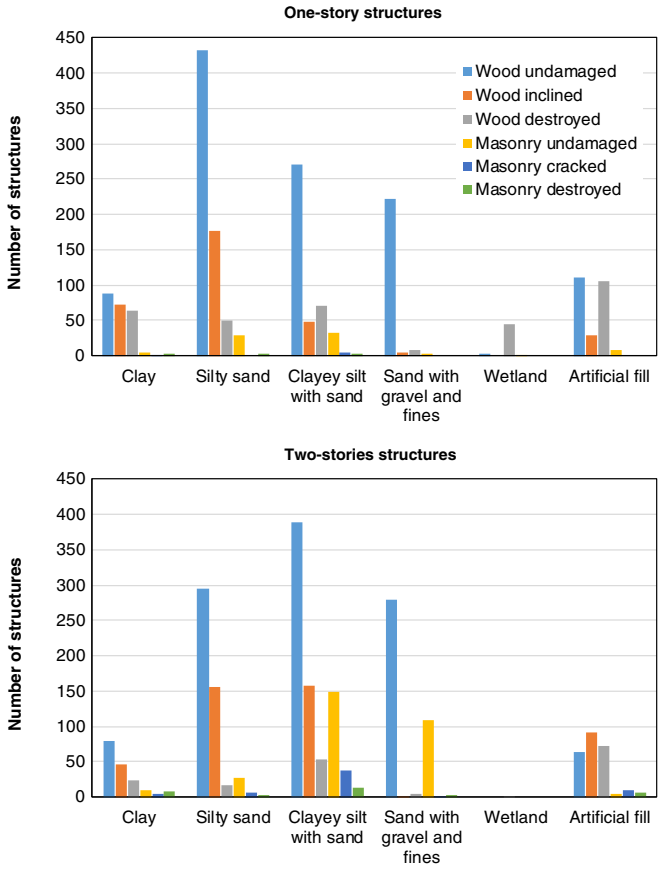

Figure 7. Number of one- and two-story structures undamaged, inclined, cracked, and destroyed during the earthquake, founded over soil types defined in the surface geology in Figure 2. The color version of this figure is available only in the electronic edition.

inclined, cracked, and destroyed. Figure 6 also shows the reinforced-concrete buildings in the city. This study considers 4022 structures, from which 65% were undamaged, 21% resulted inclined or cracked, and 14% were destroyed.

Correlation between Surface Geology and Structural Damage

Figure 7 summarizes the number of undamaged, inclined, cracked, and destroyed structures founded over the different geologic units (data provided in Table 1). Most of the damage focused on structures over the artificial fill unit: 43% of the one-story wooden houses over the artificial fill were destroyed, along with 32% of the two-story houses made of wood and masonry. The geologic unit that follows in terms of damage was the clay unit. In contrast, the unit over which the structures experienced less pronounced damage was the well-graded sand with gravel and fines. We summarize the spatial correlation between the local site conditions and the damage pattern in Figure 8, considering destroyed, inclined, cracked, and undamaged structures.

There are several outstanding examples of structures that resulted undamaged during the earthquake. For instance, the six-story reinforced-concrete Pedro de Valdivia Hotel located near the east abutment of the Pedro de Valdivia Bridge and the Prales building, a seven-story reinforced-concrete building, both located on the clayey silt with sand unit (Steinbrugge and Flores, 1963, Fig. 6). Other examples of appropriate seismic performance are the 12 wooden houses built in a German-style at the beginning of the twentieth century (locations in Fig. 5), constructed over the silty sand unit and the clayey silt with sand unit over the east bank of the Calle-Calle River (Campos, 2018). These cases are analyzed in the Discussion section.

Horizontal-to-Vertical Spectral Ratios

Ambient seismic noise measurements, 15–40 min long, were performed throughout the city of Valdivia in several campaigns using GeoSIG GVB-316 and Tromino seismometers. The criterion adopted to validate the records is that at least twenty 30 s windows were selected when the criterion of the short-term divided by long-term average ranged between 0.2 and 2.5. The signal processing was performed with the Geopsy software (Wathelet, 2005). Details of the location, duration, and the number of selected windows of each record are provided in Table S1 (available in the supplemental material to this article).

Figure 9 shows examples of the horizontal-to-vertical spectral ratios (HVSRs) obtained in different sites in the city. In the majority of the analyzed HVSR, there was a distinctive peak associated with the predominant vibration period. The large peak amplitudes of the HVSR indicate a strong impedance contrast between the sediments and the underlying metamorphic bedrock. Some HVSRs show two clear peak amplitudes, which can be attributed to a second impedance contrast, in addition to the one with the underlying bedrock.

Figure 10 interpolates the predominant periods of 92 sites in the city, showing that the distribution of predominant periods correlates neither with the surface geology nor with the damage pattern observed in Figure 8. In addition, Figures 11 and 12 show the measured predominant periods of the sites that coincide with the A–A′ and B–B′ cross sections defined in Figure 2. The change in periods along the profile apparently correlates with the geologically inferred thickness of the sediments above the bedrock.

Discussion

Despite the large earthquake magnitude, well-designed and properly constructed multistory structures at the time of the earthquake were barely damaged. The reduced damage might be explained not only by their structural redundancy (Labbé, 2019), but also by the differences in the natural periods of the structures and the predominant periods of the sites. For instance, the natural period of the reinforced-concrete Pedro de Valdivia Hotel measured in the roof deck at one end of

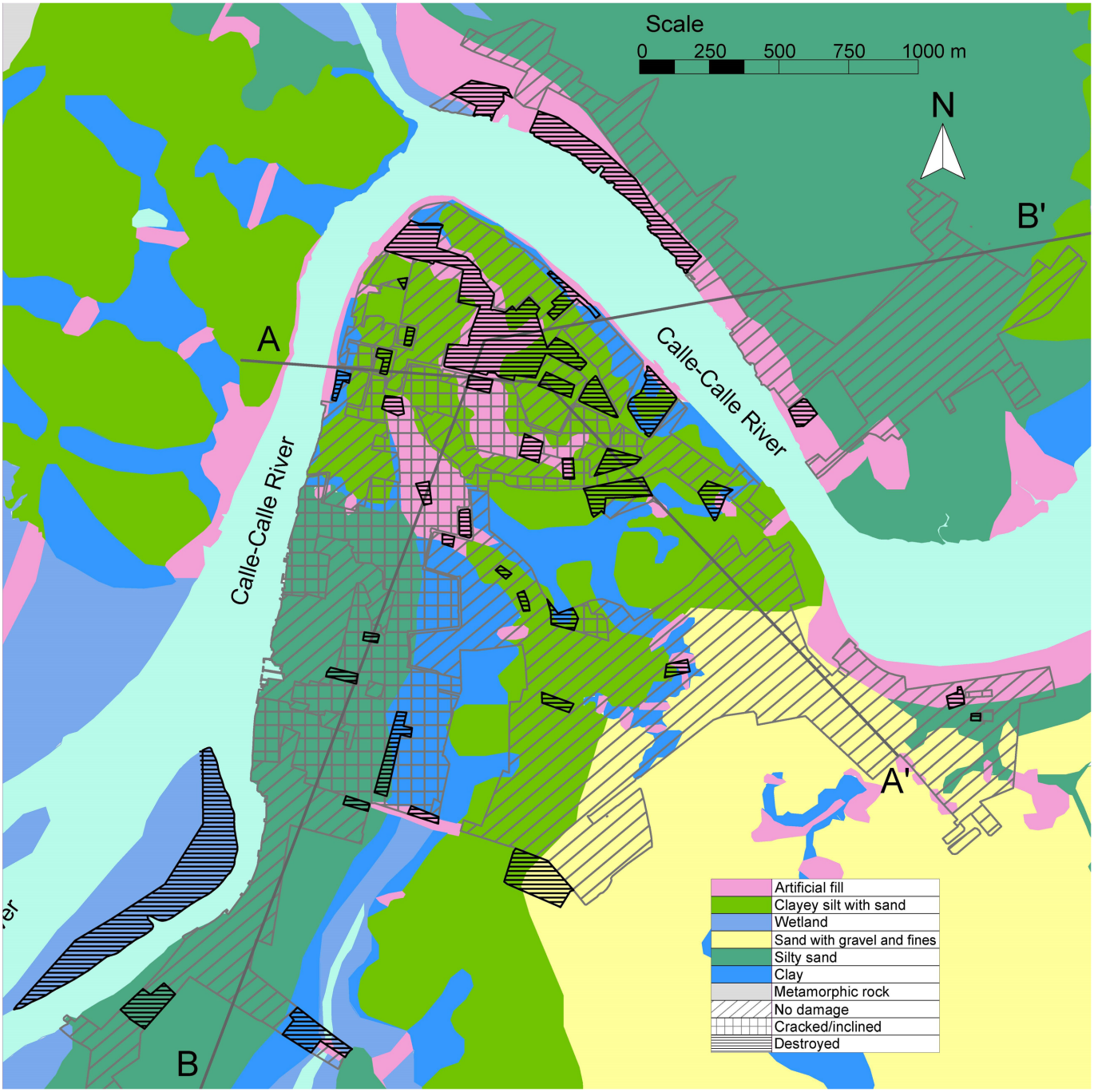

Figure 8. Correlation between surface geology and structural damage. The color version of this figure is available only in the electronic edition.

the building was $T = 0.33$ s in the long and short axes (Cloud, 1963). Recorded periods near the center of the building on the fourth floor were $T = 0.30$ s in the long axis and $T = 0.31$ s in the short axis. Another remarkable example of adequate seismic performance is the seven-story Prales building. Both structures were located over sites with predominant vibration periods between 0.9 and 1.0 s, and V_{S30} of about 210 m/s (see CSN02 profile in Fig. 4). In both cases, the natural periods of the structures were presumably shorter than the predominant periods of the sites.

The site periods of the area where the undamaged German-style wooden houses were built is between 0.8 and 1.0 s, which are also longer than the periods expected for these types of wood-frame houses. Although the V_{S30} in the sites is expected to be about 160–220 m/s, the foundation soil did not experience permanent deformations during the earthquake and they also had a proper foundation system.

Considering these observations, V_{S30} cannot be directly accounted for the damage pattern because the values reported

TABLE 1
Number of Structures Analyzed in This Study and the Underlying Geologic Unit

Type of Structure		Damage Degree	Clay	Silty Sand	Clayey Silt with Sand	Sand with Gravel	Wetland	Artificial Fill	Subtotal	Total
Wood										
	One story	Undamaged	88 (4.9)	432 (24.0)	271 (15.1)	222 (12.3)	2 (0.1)	111 (6.2)	1126 (62.6)	1798 (100)
		Inclined	73 (4.1)	177 (9.8)	48 (2.7)	4 (0.2)	0 (0)	29 (1.6)	331 (18.4)	
		Destroyed	64 (3.6)	49 (2.7)	70 (3.9)	8 (0.4)	45 (2.5)	105 (5.8)	341 (19.0)	
	Two stories	Undamaged	80 (4.6)	295 (17.1)	388 (22.4)	280 (16.2)	0 (0)	64 (3.7)	1107 (64.0)	1730 (100)
		Inclined	46 (2.7)	155 (9.0)	158 (9.1)	1 (0.1)	0 (0)	92 (5.3)	452 (26.1)	
		Destroyed	23 (1.3)	17 (1.0)	53 (3.1)	5 (0.3)	1 (0.1)	72 (4.2)	171 (9.9)	
Masonry										
	One story	Undamaged	5 (5.6)	29 (32.2)	32 (35.6)	2 (2.2)	1 (1.1)	8 (8.9)	77 (85.6)	90 (100)
		Cracked	1 (1.1)	0 (0)	4 (4.4)	0 (0)	0 (0)	0 (0)	5 (5.6)	
		Destroyed	3 (3.3)	3 (3.3)	2 (2.2)	0 (0)	0 (0)	0 (0)	8 (8.9)	
	Two stories	Undamaged	10 (2.6)	27 (7.0)	149 (38.5)	108 (27.9)	0 (0)	4 (1.0)	298 (77.0)	387 (100)
		Cracked	5 (1.3)	6 (1.6)	38 (9.8)	1 (0.3)	0 (0)	9 (2.3)	59 (15.2)	
		Destroyed	7 (1.8)	2 (0.5)	13 (3.4)	2 (0.5)	0 (0)	6 (1.6)	30 (7.8)	
Reinforced concrete										
		Undamaged	0 (0)	0 (0)	12 (70.6)	0 (0)	0 (0)	1 (5.9)	13 (76.5)	17 (100)
		Cracked	0 (0)	0 (0)	1 (5.9)	0 (0)	0 (0)	0 (0)	1 (5.9)	
		Destroyed	0 (0)	0 (0)	2 (11.8)	1 (5.9)	0 (0)	0 (0)	3 (17.6)	
Total			405	1192	1241	634	49	501	4022	

Percentages with respect to the total structures of certain material and number of stories are shown in parentheses.

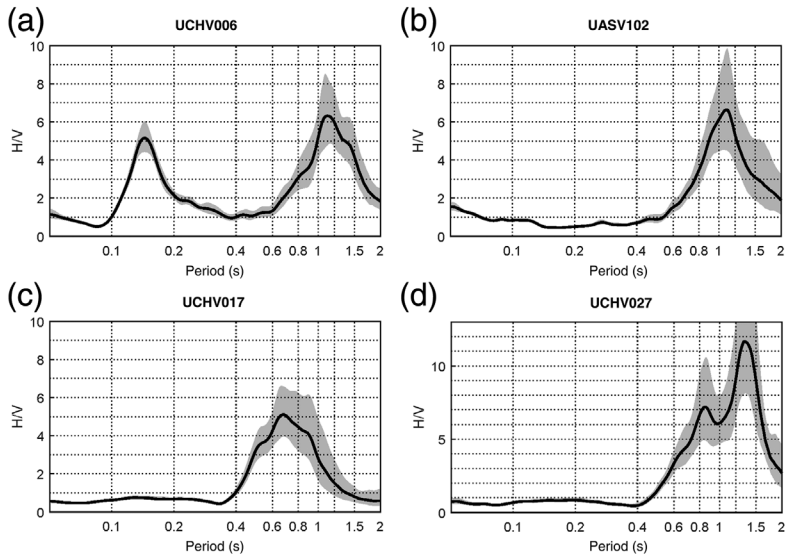

Figure 9. Examples of horizontal-to-vertical spectral ratio (HVSR) measured in the city of Valdivia. The black continuous line shows the geometric average of the 30 s windows and the gray area represents the error. Examples of (a) two-peaks, (b) long period single-peak, (c) short period single-peak, and (d) two long-period peaks HVSRs.

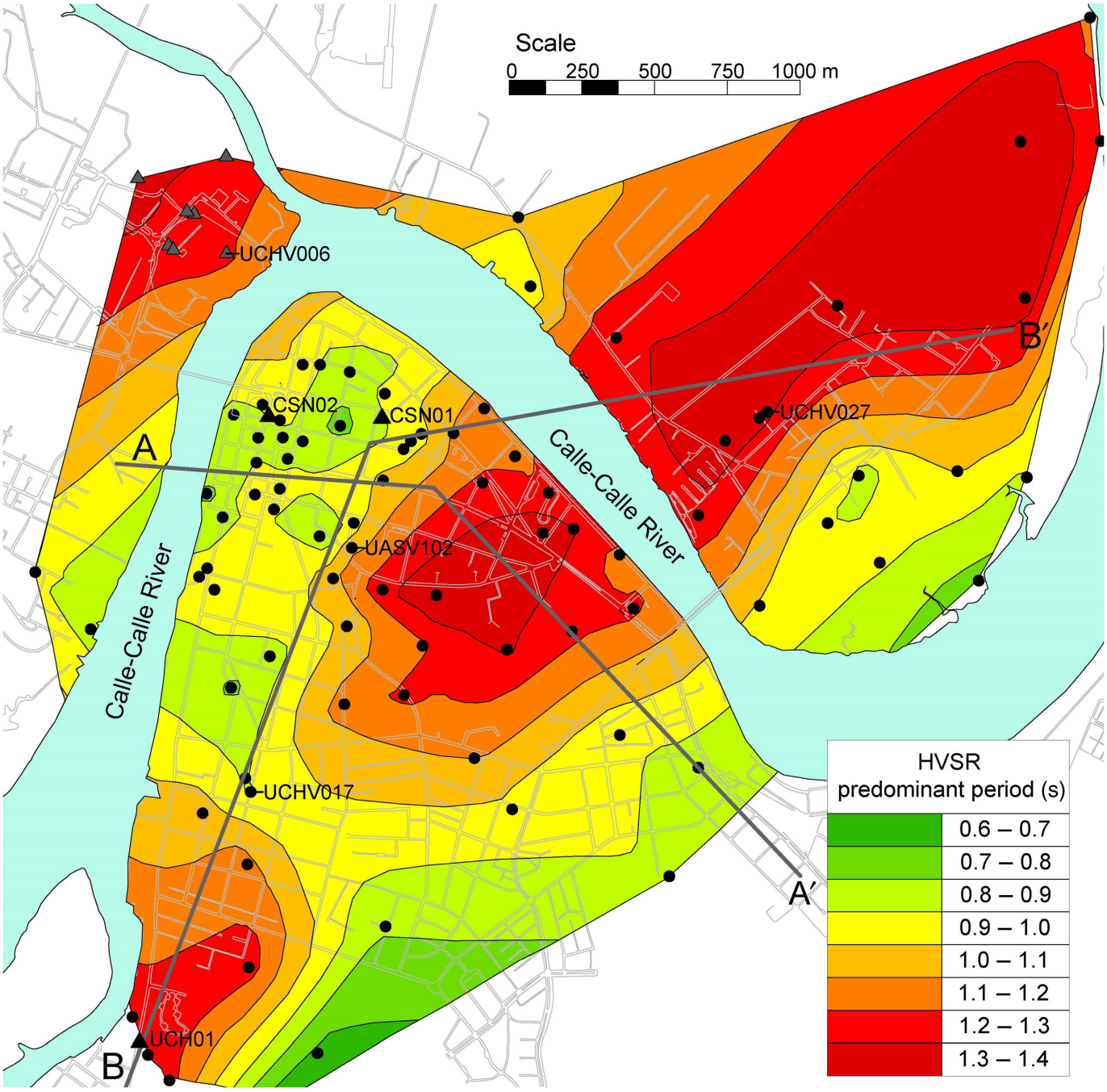

Figure 10. Interpolation of HVSR predominant vibration periods in the city of Valdivia. The color version of this figure is available only in the electronic edition.

in the study area are lower than 250 m/s and relatively constant throughout the city. On the other hand, the predominant periods from HVSR, that seem to correlate with the sediment thickness, cannot be correlated with structural damage (see the spatial relationship in Fig. S1) because the site periods are longer than the periods of the structures that experienced the earthquake.

It is worth noting that there are not available instrumental intensity measures or ground motion parameters, such as peak ground velocity, to correlate with the observed damage. On the other hand, the ground shaking during the 1960 Chile earthquake was so intense that the testimonies we could compile (see an excellent testimony of the earthquake in Labbé, 2019) suggest that the modified Mercalli intensity saturated in Valdivia as the intensity can be considered extreme (intensity X) everywhere in the city. Furthermore, estimating the local earthquake intensity in Valdivia using a standardized metrics, such as the MSK intensity, is very challenging. Although many of the structures were wood framed and were

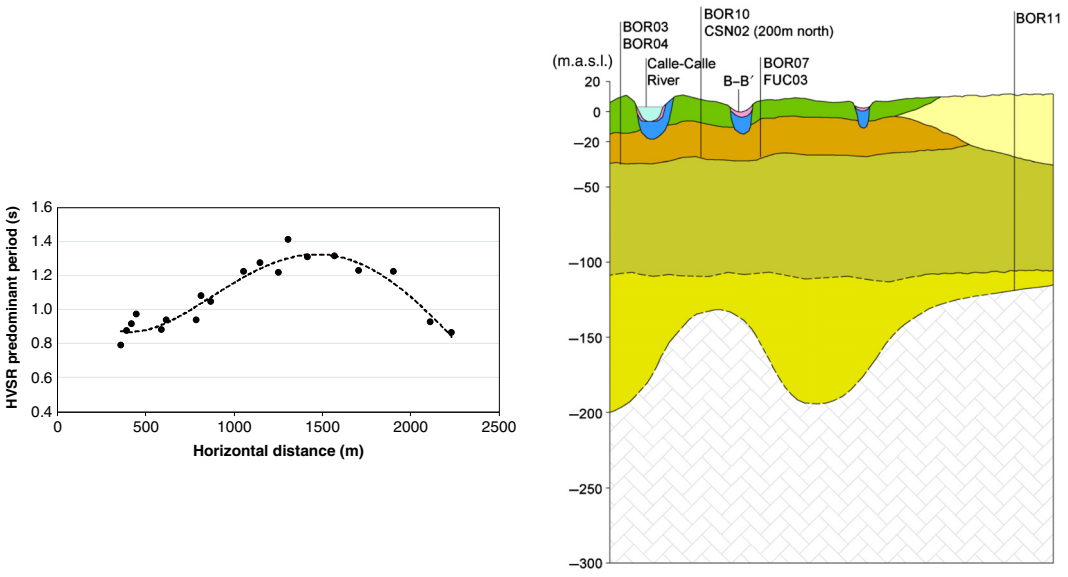

Figure 11. Cross section A–A′ along with the measured HVSR predominant vibration periods. The color version of this figure is available only in the electronic edition.

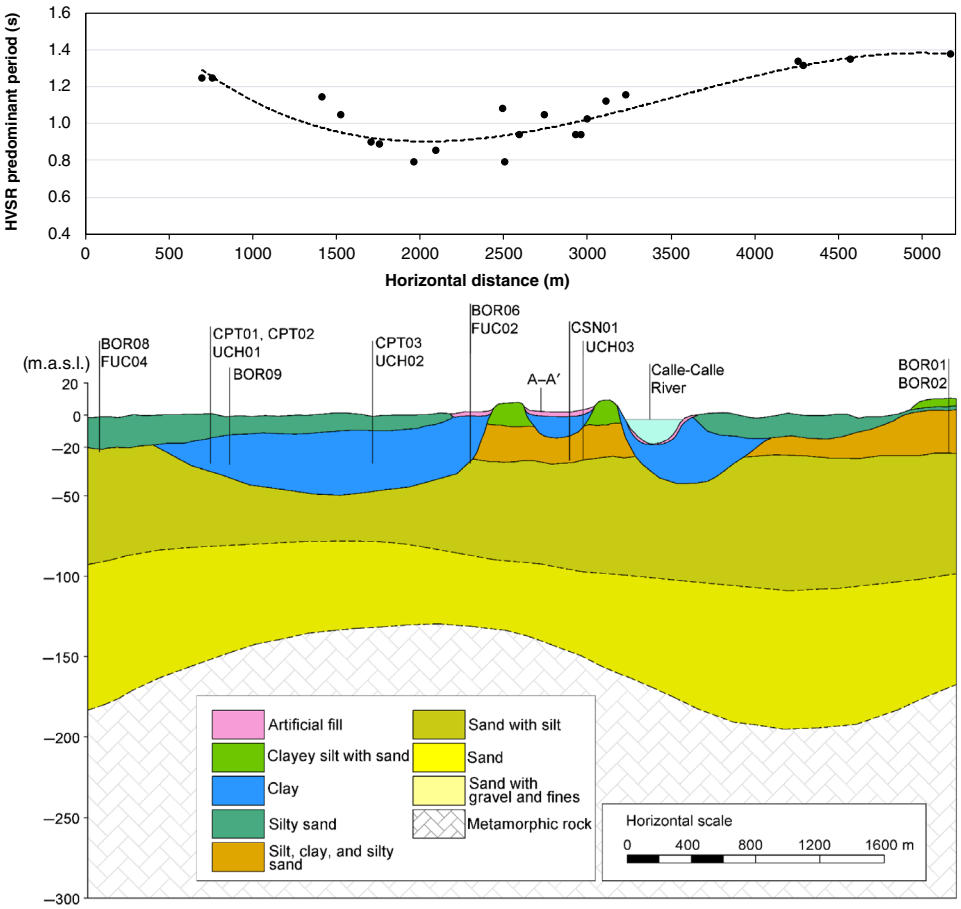

Figure 12. Cross section B–B′ along with the measured HVSR predominant vibration periods. The color version of this figure is available only in the electronic edition.

relatively well distributed over the study area, these structures were constructed following different quality standards, at different years prior the earthquake, and were built on various foundation systems. The relatively large surface geology variability in the city also complicates such task.

Conclusions

In this study, we reinterpreted the earthquake-induced damage pattern observed during the 22 May M_w 9.5 Chile earthquake and the intricate surface geology of the city of Valdivia in view of new shear-wave velocity and predominant vibration period measurements.

We found that well-constructed and founded structures were not damaged despite the large earthquake magnitude, the proximity of the city of Valdivia to the earthquake rupture area, the low shear-wave velocities measured in some of the most populated areas of the city, ranging from 150 to 250 m/s, and the long predominant vibration periods of the sites between 0.6 and 1.4 s.

In general, well-built wooden houses were sufficiently flexible to withstand intense ground motions regardless of the long predominant periods and low shear-wave velocities of the soil deposits where they were founded.

Most of the structural damage is due to deficient foundation behavior over uncontrolled backfill that experienced seismic-induced ground failures. The damage of the larger reinforced-concrete structures was due to deficiencies in design and construction. Some of the larger buildings that overcame the earthquake are still in place today in part due to their structural redundancy and the larger stiffness compared with soil deposits predominant periods.

In addition to consider the predominant period and the V_{S30} in seismic site characterization and microzonation studies, we emphasize the relevance of the shear-wave velocity and the sloping angles of the shallower soil layers that are interacting with the foundation system of one- and two-story structures because large strains of the terrain may stress and induce foundation failure.

Data and Resources

Ambient seismic noise measurements, performed by the Austral University and the University of Chile, are proprietary. The data can be released upon request to the corresponding author. The supplemental materials included with this article contains a table that details features of the ambient seismic noise records used to calculate the HVSRs in this study and a figure that shows the correlation between the predominant periods from HVSR and the earthquake-induced structural damage.

Declaration of Competing Interests

The authors acknowledge there are no conflicts of interest recorded.

Acknowledgments

Support for this research was provided by the Conicyt Fondecyt Grant Number 1190995. This article was improved thanks to the review of E. Seyhan and an anonymous reviewer.

References

Abe, K. (1979). Size of great earthquakes of 1837–1974 inferred from tsunami data, *J. Geophys. Res.* **84,** 1561, doi: 10.1029/jb084ib04p01561.

Alvarez, L. (1963). Studies made between Arauco and Valdivia with respect to the earthquake of 21 and 22 May 1960, *Bull. Seismol. Soc. Am.* **53,** 1315–1330.

American Society for Testing and Materials [ASTM] (2012). Standard test method for electronic friction cone and piezocone penetration testing of soils, *ASTM D5778-12*, doi: 10.1520/D5778-12.

Arenas, M., J. Milovic, Y. Perez, R. Troncoso, J. Behlau, J. Hanisch, and F. Helms (2005). Geología para el ordenamiento territorial: Área de Valdivia, Región de Los Lagos, Santiago, Chile (in Spanish).

Astroza, M., and R. Lazo (2010). Estudio de los daños de los terremotos del 21 y 22 de Mayo de 1960, *Congreso Chileno de Sismología e Ingeniería Antisísmica*, 441 pp. (in Spanish).

Barozzi, R., and R. Lemke (1966). Suelo de fundación de Valdivia, *Estudios Geotecnicos Number 1*, Santiago, Chile (in Spanish).

Barrientos, E., and S. N. Ward (1990). The 1960 Chile earthquake: Inversion for slip distribution from surface deformation, *Geophys. J. Int.* **103,** 589–598.

Cambiazo, C. (1961). Daños en estructuras causados por el sismo de Mayo 1960, Santiago, Chile (in Spanish).

Campos, F. (2018). Evaluación de efectos de sitio en la ciudad de Valdivia producto del Mega-Terremoto de 1960, Universidad de Chile (in Spanish).

Cifuentes, I. L. (1989). The 1960 Chilean earthquakes, *J. Geophys. Res.* **94,** 665–680.

Cisternas, M., B. F. Atwater, F. Torrejón, Y. Sawai, G. Machuca, M. Lagos, A. Eipert, C. Youlton, I. Salgado, T. Kamataki, *et al.* (2005). Predecessors of the giant 1960 Chile earthquake, *Nature* **437,** 404–407, doi: 10.1038/nature03943.

Cisternas, M., M. Carvajal, R. Wesson, L. L. Ely, and N. Gorigoitia (2017). Exploring the historical earthquakes preceding the giant 1960 Chile earthquake in a time-dependent seismogenic zone, *Bull. Seismol. Soc. Am.* **107,** 2664–2675, doi: 10.1785/0120170103.

Cloud, W. K. (1963). Period measurements of structures in Chile, *Bull. Seismol. Soc. Am.* **53,** 359–379.

Cox, D. C., and J. F. Mink (1963). The tsunami of 23 May 1960 in the Hawaiian Islands, *Bull. Seismol. Soc. Am.* **53,** 1191–1209.

Doyel, W., A. Moraga, and E. Falcon (1963). Relation between the geology of Valdivia, Chile, and the damage produced by the earthquake of 22 May 1960, *Bull. Seismol. Soc. Am.* **53,** 1331–1345.

Duke, M., and D. Leeds (1963). Response of soils, foundations, and earth structures to Chilean earthquakes of 1960, *Bull. Seismol. Soc. Am.* **53,** 309–357.

Fujii, Y., and K. Satake (2013). Slip distribution and seismic moment of the 2010 and 1960 Chilean earthquakes inferred from tsunami waveforms and coastal geodetic data, *Pure Appl. Geophys.* **170,** 1493–1509, doi: 10.1007/s00024-012-0524-2.

Galli, C., and J. Sánchez (1963a). Effects of the earthquakes of May 1960 in Concepcion and vicinity, *Bull. Seismol. Soc. Am.* **53,** 1281–1297.

Galli, C., and J. Sánchez (1963b). Relation between geology and the effects of the earthquakes of May 1960 in the city of Castro and vicinity, Chiloé, *Bull. Seismol. Soc. Am.* **53,** 1263–1271.

Galli, C., and J. Sánchez (1963c). Relation between the geology and the effects of the earthquakes of May 1960 in the city of Ancud and vicinity, Chiloé, *Bull. Seismol. Soc. Am.* **53,** 1273–1280.

Ho, T. C., K. Satake, S. Watada, and Y. Fujii (2019). Source estimate for the 1960 Chile earthquake from joint inversion of geodetic and transoceanic tsunami data, *J. Geophys. Res.* **124,** 2812–2828, doi: 10.1029/2018JB016996.

Instituto Nacional de Normalización [INN] (2012). Earthquake resistant design of buildings, NCh 433 of 1996, Modified in 2012, Santiago, Chile.

Kanamori, H. (1977). The energy release in great earthquake, *J. Geophys. Res.* **82,** 2981–2987.

Kanamori, H., and J. J. Cipar (1974). Focal process of the Great Chilean earthquake May 22, 1960, *Phys. Earth Planet. In.* **9,** 128–136, doi: 10.1016/B978-0-12-205750-2.50005-0.

Keys, J. G. (1963). The tsunami of 22 May 1960, in the Samoa and Cook Islands, *Bull. Seismol. Soc. Am.* **53,** 1211–1227.

Labbé, R. (2019). Valdivia 1960 M_w 9.5 A testimony of my own, *XII Congreso Chileno de Sismologia e Ingenieria Sismica*, 1–12.

Lástrico, R. (1967). Relación entre los daños en los terremotos de 1960 y los suelos de fundación de Valdivia, Universidad de Chile (in Spanish).

Leyton, F., A. Leopold, G. Hurtado, C. Pastén, S. Ruiz, G. Montalva, and E. Saéz (2018). Geophysical characterization of the Chilean seismological stations: First results, *Seismol. Res. Lett.* **89,** 519–525, doi: 10.1785/0220170156.

Moreno, M. S., J. Bolte, J. Klotz, and D. Melnick (2009). Impact of megathrust geometry on inversion of coseismic slip from geodetic data: Application to the 1960 Chile earthquake, *Geophys. Res. Lett.* **36,** 1–5, doi: 10.1029/2009GL039276.

Ojeda, J., S. Ruiz, F. del Campo, and M. Carvajal (2020). The 21 May 1960 M_w 8.1 Concepción earthquake: A deep megathrust foreshock that started the 1960 central-south Chilean seismic sequence, *Seismol. Res. Lett.* **91,** 1617–1627, doi: 10.1785/0220190143.

Pastén, C., M. Sáez, S. Ruiz, F. Leyton, J. Salomón, and P. Poli (2016). Deep characterization of the Santiago Basin using HVSR and cross-correlation of ambient seismic noise, *Eng. Geol.* **201,** 57–66, doi: 10.1016/j.enggeo.2015.12.021.

Plafker, G., and J. C. Savage (1970). Mechanism of the Chilean earthquakes of May 21 and 22, 1960, *Geol. Soc. Am. Bull.* **81,** 1001–1030.

Press, F., A. Ben-Menahem, and M. N. Toksoz (1961). Experimental determination of earthquake fault length and rupture velocity, *J. Geophys. Res.* **66,** 3471–3485.

Ruiz, S., and R. Madariaga (2018). Historical and recent large megathrust earthquakes in Chile, *Tectonophysics* **733,** 37–56, doi: 10.1016/j.tecto.2018.01.015.

Saint-Amand, P. (1961a). Observaciones e interpretacion de los terremotos de 1960, 136, 23–42 (in Spanish).

Saint-Amand, P. (1961b). *Los terremotos de Mayo – Chile 1960*, China Lake, California (in Spanish).

Sievers, H. A., G. Villegas, and G. Barros (1963). The seismic sea wave of 22 May 1960 along the Chilean coast, *Bull. Seismol. Soc. Am.* **53,** 1125–1190.

Steinbrugge, K. V., and R. Flores (1963). The Chilean earthquakes of May 1960: A structural engineering viewpoint, *Bull. Seismol. Soc. Am.* **53,** 225–307.

Thomas, B. Y. H., W. Bowes, and N. Bravo (1963a). Field observations made between Puerto Montt and Maullin, *Bull. Seismol. Soc. Am.* **53,** 1353–1356.

Thomas, B. Y. H., W. Bowes, and N. Bravo (1963b). Geologic report on the effects of the earthquake of 22 May 1960 in the city of Puerto Varas, *Bull. Seismol. Soc. Am.* **53,** 1347–1352.

Thomas, H., W. Bowes, and N. Bravo (1963). Geologic report on the effects of the earthquake of 22 May 1960 on the city Llanquihue, *Bull. Seismol. Soc. Am.* **53,** 1357–1360.

Vega, R. M., M. Mella, S. N. Nielsen, and M. Pino (2018). Stratigraphy and sedimentology of a late Pleistocene incised valley fill: A depositional and paleogeographic model for "Cancagua" deposits in north-western Patagonia, Chile, *Andean Geol.* **45,** 161, doi: 10.5027/andgeov45n2-3030.

Vitousek, M. J. (1963). The tsunami of 22 May 1960 in French Polynesia, *Bull. Seismol. Soc. Am.* **53,** 1229–1236.

Watanabe, T., and J. C. Karzulovic (1960). Los movimientos sísmicos del mes de mayo de 1960 en Chile, *Anales de la Facultad de Ciencias Físicas y Matemáticas* **17,** 41–87 (in Spanish).

Wathelet, M. (2005). Geopsy geophysical signal database for noise array processing, Software, LGIT, Grenoble, France.

Weischet, W. (1963). The distribution of the damage caused by the earthquake in Valdivia in relation to the form of the terrane, *Bull. Seismol. Soc. Am.* **53,** 1259–1262.

Manuscript received 19 October 2019
Published online 5 May 2021